

Agonist-Independent Constitutive Activity of Angiotensin II Receptor Promotes Cardiac Remodeling in Mice

Noritaka Yasuda, Hiroshi Akazawa, Kaoru Ito, Ippei Shimizu, Yoko Kudo-Sakamoto, Chizuru Yabumoto, Masamichi Yano, Rie Yamamoto, Yukako Ozasa, Tohru Minamino, Atsuhiko T. Naito, Toru Oka, Ichiro Shiojima, Kouichi Tamura, Satoshi Umemura, Mona Nemer, Issei Komuro

See Editorial Commentary, pp 542–544

Abstract—The angiotensin II (Ang II) type 1 (AT₁) receptor mainly mediates the physiological and pathological actions of Ang II, but recent studies have suggested that AT₁ receptor inherently shows spontaneous constitutive activity even in the absence of Ang II in culture cells. To elucidate the role of Ang II-independent AT₁ receptor activation in the pathogenesis of cardiac remodeling, we generated transgenic mice overexpressing AT₁ receptor under the control of α -myosin heavy chain promoter in angiotensinogen-knockout background (AT₁Tg-AgtKO mice). In AT₁Tg-AgtKO hearts, redistributions of the G α_{q11} subunit into cytosol and phosphorylation of extracellular signal-regulated kinases were significantly increased, compared with angiotensinogen-knockout mice hearts, suggesting that the AT₁ receptor is constitutively activated independent of Ang II. As a consequence, AT₁Tg-AgtKO mice showed spontaneous systolic dysfunction and chamber dilatation, accompanied by severe interstitial fibrosis. Progression of cardiac remodeling in AT₁Tg-AgtKO mice was prevented by treatment with candesartan, an inverse agonist for the AT₁ receptor, but not by its derivative candesartan-7H, deficient of inverse agonism attributed to a lack of the carboxyl group at the benzimidazole ring. Our results demonstrate that constitutive activity of the AT₁ receptor under basal conditions contributes to the cardiac remodeling even in the absence of Ang II, when the AT₁ receptor is upregulated in the heart. (*Hypertension*. 2012;59:627-633.) • Online Data Supplement

Key Words: ARB ■ cardiac dysfunction ■ fibrosis ■ G protein-coupled receptor ■ inverse agonist

The angiotensin II (Ang II) type 1 (AT₁) receptor is a 7 transmembrane spanning G protein-coupled receptor (GPCR), and the activation of AT₁ receptor is involved in regulating pathophysiological processes of the cardiovascular system. In principle, the AT₁ receptor is activated on binding to Ang II, which is produced systemically or locally after sequential proteolytic processing. However, recent studies demonstrated that the AT₁ receptor inherently shows spontaneous constitutive activity even in the absence of Ang II in cultured cells.^{1–3} GPCRs are structurally unstable and show significant levels of spontaneous activity in an agonist-independent manner.⁴ In addition, we and others demonstrated that the AT₁ receptor can be activated by mechanical stress independent of Ang II^{5–7} through conformational switch of the receptor.¹ These observations have highlighted

the inverse agonist activity of AT₁ receptor blockers (ARBs) as a drug-specific property that can inhibit Ang II-independent constitutive activity and mechanical stress-induced receptor activation.^{1,2,5,8} In a mouse model, mechanical stress-induced AT₁ receptor activation led to the development of cardiac hypertrophy independent of Ang II, and treatment with inverse agonists for the AT₁ receptor-attenuated cardiac hypertrophy thus formed.⁵ However, the pathogenic role of Ang II-independent constitutive activity of the AT₁ receptor and clinical relevance of inverse agonist activity of ARBs against constitutive receptor activation remains to be elucidated in vivo. In several GPCRs, gain-of-function mutations are causative of diseases, but any activating mutations in the coding region of the AT₁ receptor gene have not been identified in hypertension or primary hyperaldosteronism.^{9,10}

Received April 24, 2011; first decision May 23, 2011; revision accepted January 6, 2012.

From the Department of Cardiovascular Science and Medicine (N.Y., K.I., Ip.S., R.Y., Y.O., T.M.), Chiba University Graduate School of Medicine, Chiba, Japan; Departments of Cardiovascular Medicine (H.A., Y.K.-S., C.Y., M.Y., T.O., I.K.) and Cardiovascular Regenerative Medicine (A.T.N., Ic.S.), Osaka University Graduate School of Medicine, Suita, Japan; Department of Medical Science and Cardiorenal Medicine (K.T., S.U.), Yokohama City University Graduate School of Medicine, Yokohama, Japan; Laboratory of Cardiac Growth and Differentiation (M.N.), Department of Biochemistry, Microbiology, and Immunology, Faculty of Medicine, University of Ottawa, Ottawa, Ontario, Canada.

The online-only Data Supplement is available with this article at <http://hyper.ahajournals.org/lookup/suppl/doi:10.1161/HYPERTENSIONAHA.111.175208/-/DC1>.

Correspondence to Issei Komuro, Department of Cardiovascular Medicine, Osaka University Graduate School of Medicine, 2-2 Yamadaoka, Suita, Osaka 565-0871, Japan. E-mail komuro-ty@umin.ac.jp

© 2012 American Heart Association, Inc.

Hypertension is available at <http://hyper.ahajournals.org>

DOI: 10.1161/HYPERTENSIONAHA.111.175208

Although knock-in mice with a constitutively activating mutation (substitution of Asn¹¹¹ to Ser with a C-terminal deletion) showed low-renin hypertension and progressive fibrosis in kidney and heart,¹¹ it remains unclear whether constitutive activity of the native AT₁ receptor leads to some phenotypic abnormalities even under circumstances where the production of Ang II is genetically inhibited.

Therefore, we generated transgenic mice overexpressing AT₁ receptor under the control of α -myosin heavy chain promoter in the *angiotensinogen* (*Agt*)-knockout background. Here, we show that constitutive activity of the AT₁ receptor indeed contributes to cardiac remodeling independent of Ang II even in vivo, when the AT₁ receptor is upregulated in the heart.

Methods

An expanded Methods section is available in the online-only Data Supplement.

Mice, Transverse Aortic Constriction Operation, and Transthoracic Echocardiography

Mice expressing the human *AGTR1a* gene under the control of α -myosin heavy chain promoter (on the C57BL/6J background) and mice deficient for the *Agt* gene (on the Institute of Cancer Research [ICR] background) were described previously.^{12,13} Candesartan cilexetil and candesartan-7H were synthesized by Takeda Pharmaceutical Co, Ltd, and administered via drinking water. Sham or transverse aortic constriction operation was performed as described previously,⁵ and transthoracic echocardiography was performed on conscious mice with a Vevo 770 Imaging System. All of the protocols were approved by the institutional animal care and use committee of Chiba University.

Ang II Infusion and BP Measurement

Eight-week-old C57BL/6J male mice were treated with Ang II (0.6 mg/kg per day) or vehicle for 2 weeks using an osmotic mini-pump (ALZET model 2002; Durent Corp). The BP and pulse rates were measured noninvasively by a programmable sphygmomanometer (BP-98A, Softron) using the tail-cuff method.

Real-Time RT-PCR Analysis

Total RNA was extracted by using the RNeasy kit (Qiagen), and single-stranded cDNA was transcribed by using QuantiTect Reverse Transcription kit (Qiagen), according to the manufacturer's protocol. We conducted quantitative real-time PCR analysis with the Universal ProbeLibrary Assays (Roche Applied Science), according to the manufacturer's instructions.

Western Blot Analysis and Histological Analysis

Western blot analysis and histological were performed as described previously.^{1,5}

Radioligand Receptor Binding Assay

Radioligand binding assays were performed as described previously.^{1,14}

Statistics

All of the data are presented as mean \pm SEM. Two-group comparison was analyzed by unpaired 2-tailed Student *t* test, and multiple-group comparison was performed by 1-way ANOVA followed by the Fisher protected least significant difference test for comparison of means. A *P* value of *P* < 0.05 was considered to be statistically significant.

Results

AT₁ Receptor Is Constitutively Activated Without the Involvement of Ang II in AT₁ Transgenic-Angiotensinogen Knockout Mice Hearts

To elucidate the pathogenic role of Ang II-independent AT₁ receptor activation in the hearts, we crossed transgenic mice overexpressing human AT₁ receptor under the control of cardiac-specific α -myosin heavy chain promoter (AT₁Tg) with angiotensinogen knockout mice (AgtKO) to generate AT₁Tg-AgtKO mice. First, we examined the expression levels of renin-angiotensin system components. Although the mRNA level of the AT₂ receptor (*Agtr2*) was significantly higher in AT₁Tg-AgtKO hearts than in AgtKO hearts, there was no significant difference in protein levels of the AT₂ receptor between AT₁Tg-AgtKO and AgtKO hearts (Figure S1 in the online-only Data Supplement). Furthermore, the mRNA levels of the AT_{1b} receptor (*Agtr1b*), angiotensin-converting enzyme (*Ace*), and renin (*Ren1* and *Ren2*) did not differ significantly between AT₁Tg-AgtKO and AgtKO hearts (Figure S1A).

We next determined the density of the AT₁ receptor (B_{\max} values of receptor binding) in membranes isolated from the ventricles of AgtKO and AT₁Tg-AgtKO mice by radioligand binding assays using ¹²⁵I-[Sar¹, Ile⁸] Ang II as ligand. Consistent with the previous report,¹² the B_{\max} of AT₁ receptor was increased by >200-fold in AT₁Tg-AgtKO hearts compared with AgtKO hearts (AT₁Tg-AgtKO: 5.41 \pm 1.79 pmol/mg of protein; AgtKO: 24.0 \pm 13.9 fmol/mg of protein; *n* = 4 per group; *P* < 0.01). Next, to evaluate whether the AT₁ receptor is constitutively activated in the AT₁Tg-AgtKO hearts, we examined redistribution of G α_{q11} into the cytosolic fraction and phosphorylation of extracellular signal-regulated kinases (ERKs) in AgtKO and AT₁Tg-AgtKO hearts. On activation of the AT₁ receptor, the heterotrimeric G_q protein dissociates into α and $\beta\gamma$ subunits, and the GTP-bound G α_q subunit stimulates diverse intracellular signaling pathways, including the ERK pathway.^{15,16} Redistribution of G α_{q11} subunits from the particulate to the cytosolic fraction was significantly increased in AT₁Tg-AgtKO hearts compared with AgtKO hearts (Figure 1A). In addition, the levels of phosphorylated ERKs in AT₁Tg-AgtKO hearts was significantly increased compared with AgtKO hearts (Figure 1B). These results suggest that the AT₁ receptor is upregulated and constitutively activated without the involvement of Ang II in the AT₁Tg-AgtKO hearts.

AT₁Tg-AgtKO Mice Display Progressive Cardiac Remodeling

Tail-cuff measurements of systolic and diastolic blood pressure (BPs) and pulse rates revealed that these parameters did not differ significantly between AgtKO and AT₁Tg-AgtKO mice at 20 weeks of age (Table). However, morphological and physiological analysis revealed progressive chamber dilatation, contractile dysfunction, and interstitial fibrosis in AT₁Tg-AgtKO mice, whereas cardiac structure and function were normal in AgtKO mice. At 20 weeks of age, AT₁Tg-AgtKO mice displayed \approx 1.5-fold increase in heart:body

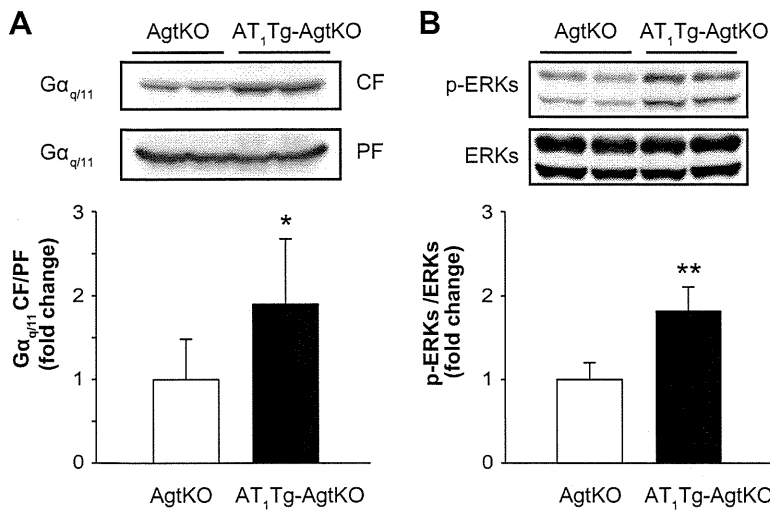


Figure 1. Constitutive activation of angiotensin II type 1 (AT₁) receptor in AT₁ transgenic (AT₁Tg)-angiotensinogen-knockout (AgtKO) hearts. **A**, Immunoblot analysis of Gα_{q/11} in cytosolic fraction (CF) and particulate fraction (PF) extracted from AgtKO (n=6) and AT₁Tg-AgtKO (n=6) hearts. The quantitation of the Gα_{q/11} in CF/PF is shown as a bar graph. Data are presented as mean±SEM. *P<0.05 vs AgtKO mice. **B**, Immunoblot analysis of phosphorylated extracellular signal-regulated kinases (ERKs; p-ERKs) and total ERKs in AgtKO (n=8) and AT₁Tg-AgtKO (n=8) hearts. The quantitation of the p-ERKs/ERKs is shown as a bar graph. Data are presented as mean±SEM. **P<0.01 vs AgtKO mice.

weight ratio compared with AgtKO mice (Table). Echocardiographic examination revealed a progressive increase in left ventricular end-diastolic dimension and decrease in the percentage of fractional shortening (Figure 2A). Histologically, a significant increase in interstitial fibrosis was observed in AT₁Tg-AgtKO mice at 20 weeks of age and further exacerbated at 36 weeks of age (Figure 2B). Furthermore, real-time RT-PCR indicated that mRNA levels of fetal cardiac genes (*Nppa*, *Nppb*, and *Acta1*) and extracellular matrix genes (*Col3a1* and *Postn*) were significantly increased in AT₁Tg-AgtKO hearts compared with AgtKO hearts (Figure 2C). These results indicate that upregulation of the AT₁ receptor induced spontaneous and progressive cardiac remodeling in AT₁Tg-AgtKO mice in spite of systemic deficiency of Ang II.

Cardiac Remodeling in AT₁Tg-AgtKO Mice Is Prevented by Treatment With an Inverse Agonist for the AT₁ Receptor

We examined whether an AT₁ receptor blocker candesartan could prevent the progression of cardiac remodeling in AT₁Tg-AgtKO mice. In cultured cells, candesartan reduces the basal activity of both the wild-type AT₁ receptor and constitutively active AT₁ mutant receptors, suggesting that candesartan is an inverse agonist for the AT₁ receptor.¹ Candesartan also suppresses mechanical stretch-induced he-

lical movement and thereby inhibits receptor activation¹ and prevents pressure-overload cardiac hypertrophy in mice.⁵

Tail-cuff measurements revealed a significant increase in systolic BP in 8-week-old C57BL/6 male mice treated with Ang II (0.6 mg/kg per day) for 2 weeks using an osmotic minipump (Figure 3A). This BP elevation was abolished by treatment with candesartan cilexetil (1 mg/kg per day) in drinking water. Candesartan cilexetil is a prodrug that is converted rapidly and completely to candesartan during gastrointestinal absorption.¹⁷ Interestingly, treatment with candesartan cilexetil prevented the progression of cardiac remodeling in AT₁Tg-AgtKO mice, when treatment was initiated at 6 weeks of age. The increases in heart:body weight ratio (Figure 3B), chamber dilatation and contractile dysfunction (Figure 3C), and interstitial fibrosis (Figure 3D) were significantly attenuated by candesartan cilexetil. Consistently, real-time RT-PCR indicated that the increases in mRNA levels of fetal cardiac genes (*Nppa*, *Nppb*, and *Acta1*) and extracellular matrix genes (*Col3a1* and *Postn*) in AT₁Tg-AgtKO hearts were significantly attenuated by treatment with candesartan cilexetil (Figure 3E).

We reported previously that tight binding between the carboxyl group of candesartan and specific residues of the AT₁ receptor was critical for the potent inverse agonism and that a derivative of candesartan (candesartan-7H), lacking the carboxyl group at the benzimidazole ring, could not suppress agonist-independent activities of the receptor.¹ Although treatment with candesartan-7H (1 mg/kg per day) had no effect, treatment with candesartan-7H (20 mg/kg per day) suppressed Ang II-induced BP elevation in C57BL/6 male mice, almost equally as treatment with candesartan cilexetil (1 mg/kg per day) did. (Figure 3A). However, treatment with candesartan-7H (20 mg/kg per day) did not prevent the increase in heart:body weight ratio (Figure 3B), progression of chamber dilatation, contractile dysfunction (Figure 3C), interstitial fibrosis (Figure 3D), or the increase in mRNA levels of fetal cardiac genes and extracellular matrix genes in AT₁Tg-AgtKO mice. Tail-cuff measurements revealed that treatment with candesartan cilexetil and candesartan-7H did not change systolic BP in AT₁Tg-AgtKO mice (Figure S2)

Table. Measurement of Heart Weight, Heart Rate, and BP in AgtKO and AT₁Tg-AgtKO Mice at 20 wk of Age

Parameters	AgtKO	No.	AT ₁ Tg-AgtKO	No.
BW, g	31.0±3.4	9	30.2±3.5	6
HW/BW, mg/g	3.48±0.25	9	5.08±0.19*	6
HR, bpm	556.0±85.3	6	540.1±55.0	6
Systolic BP, mm Hg	83.4±8.8	6	85.9±3.7	6
Diastolic BP, mm Hg	57.3±6.0	6	55.7±7.4	6
Mean BP, mm Hg	65.7±5.3	6	66.0±5.0	6

BW indicates body weight; HR, heart rate; HW/BW, heart:body weight ratio; BP, blood pressure; AgtKO, angiotensinogen-knockout; AT₁Tg, angiotensin II type 1 transgenic.

*P<0.01 vs sham.

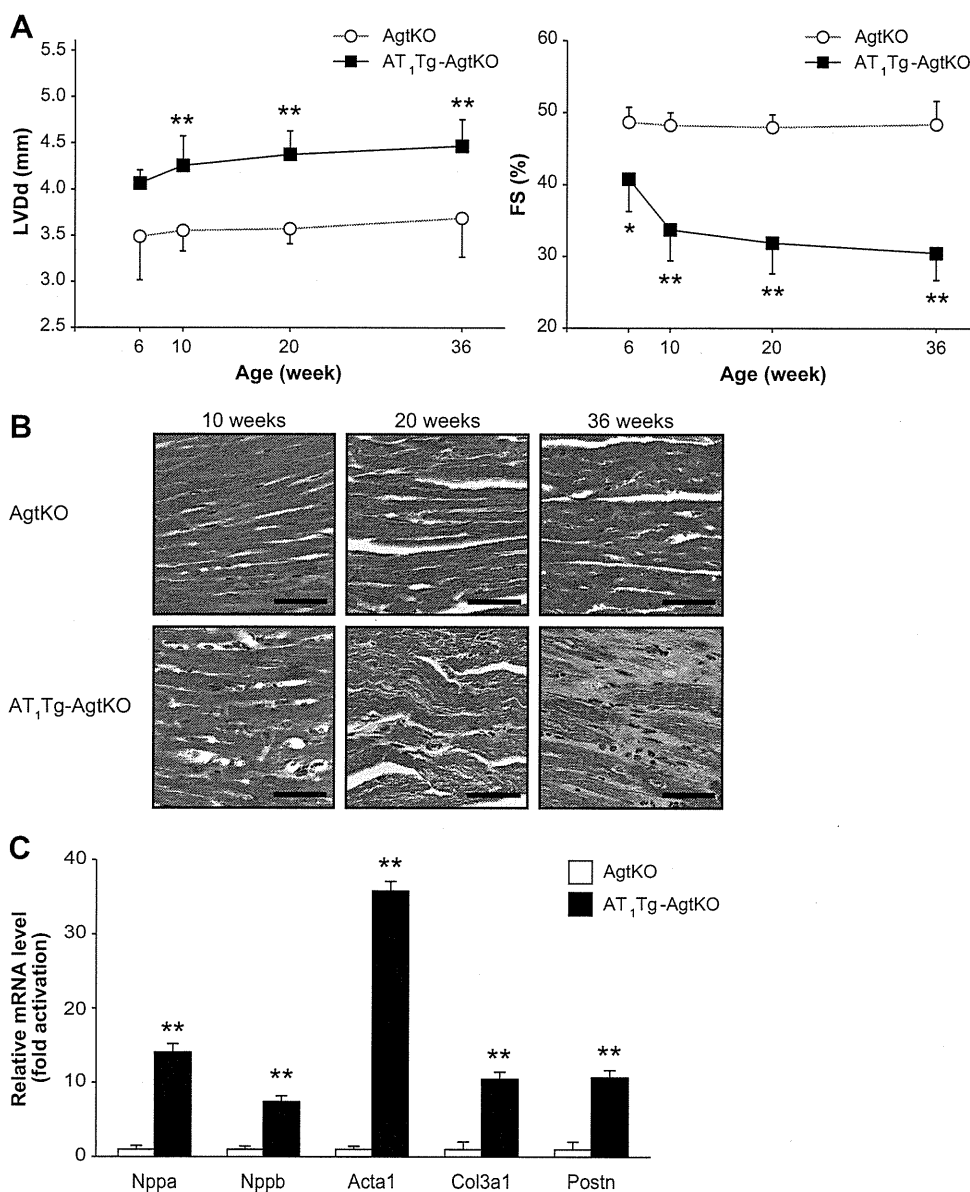


Figure 2. Spontaneous development of cardiac remodeling in angiotensin II type 1 (AT₁) transgenic (AT₁Tg)-angiotensinogen-knockout (AgtKO) mice. **A**, Left ventricular end-diastolic dimension (LVDD) and fractional shortening (FS) of AgtKO (n=7–9) and AT₁Tg-AgtKO (n=9–11) mice measured by echocardiogram at 6, 10, 20, and 36 weeks of age. Data are presented as mean±SEM. **P*<0.05, ***P*<0.01 vs AgtKO mice. ○, AgtKO; ■, AT₁Tg-AgtKO. **B**, Histological sections with Masson trichrome staining of AgtKO and AT₁Tg-AgtKO hearts at 10, 20, and 36 weeks of age. Scale bars, 50 μm. **C**, The mRNA expressions of cardiac genes *Nppa*, *Nppb*, and *Acta1*, and extracellular matrix genes *Col3a1* and *Postn* in AgtKO (n=9) and AT₁Tg-AgtKO (n=9) hearts at 10 weeks of age. □, AgtKO; ■, AT₁Tg-AgtKO. Data are presented as mean±SEM. ***P*<0.01 vs AgtKO mice.

because Ang II is not produced in AT₁Tg-AgtKO mice. Collectively, these results suggest that cardiac remodeling in AT₁Tg-AgtKO mice was prevented by candesartan, an inverse agonist for the AT₁ receptor, but not by candesartan-7H, which cannot inhibit Ang II-independent AT₁ receptor activation because of a lack of inverse agonist activity.

Discussion

In several GPCRs, the constitutive activity is closely related to physiological function. For example, constitutive activity of the histamine H₃ receptor controls histaminergic neuron activity in rodents.¹⁸ The melanocortin-4 receptor and growth hormone secretagogue receptor have high constitutive activ-

ity, and loss of constitutive activity in mutant melanocortin-4 receptors or growth hormone secretagogue receptors leads to obesity or short stature in humans, respectively.^{19,20} In contrast, constitutively active mutations in several GPCRs give rise to diseases in humans. For example, somatic mutations of thyrotropin-stimulating hormone receptor or luteinizing hormone receptor lead to hyperfunctioning thyroid adenoma or male precocious puberty, respectively.^{21,22}

In the present work, we provide experimental evidence that transgenic myocardial overexpression of the wild-type AT₁ receptor increases constitutive activity of the receptor, leading to cardiac enlargement, interstitial fibrosis, and contractile dysfunction, even in the absence of Ang II. To exclude a

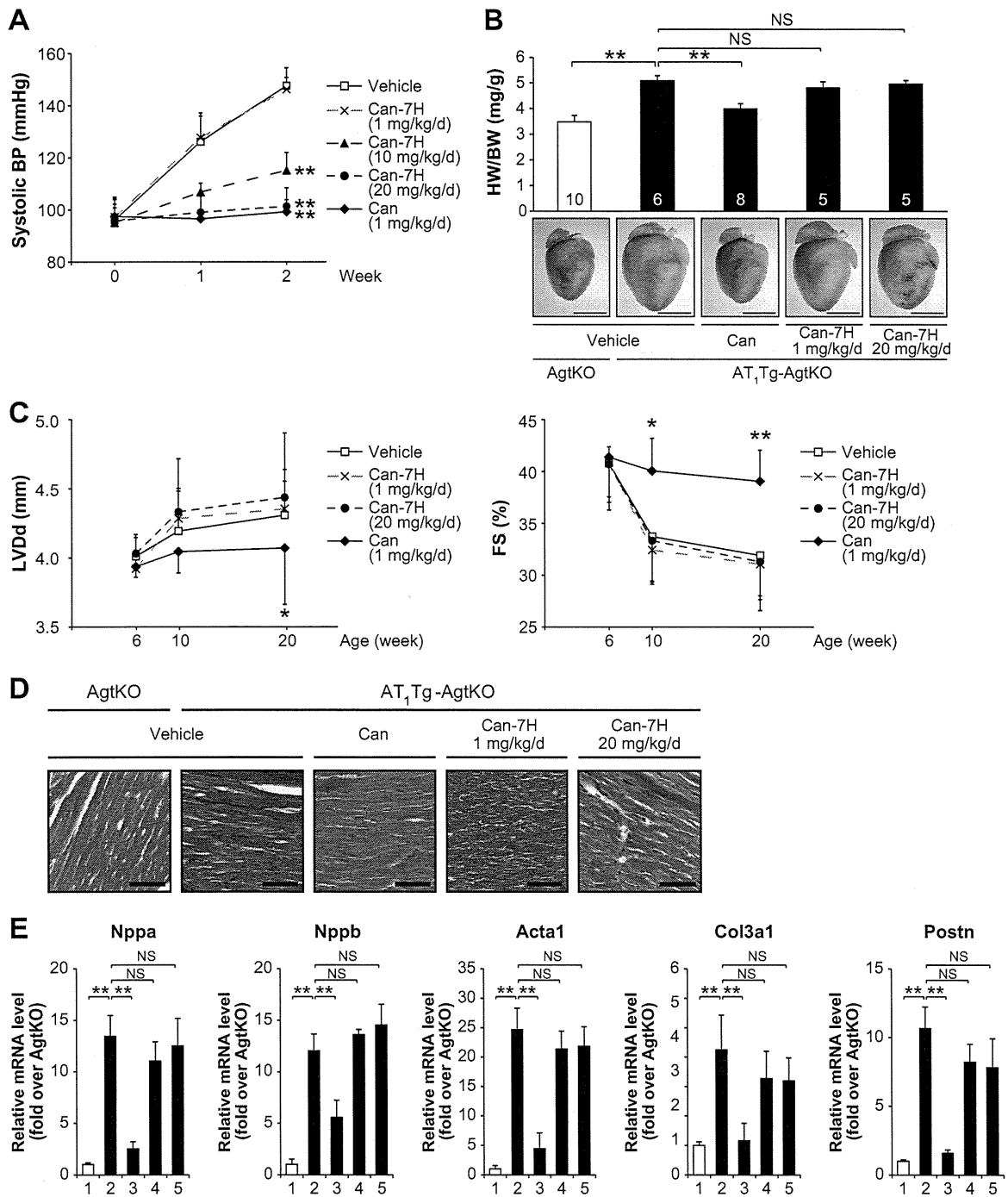


Figure 3. Prevention of cardiac remodeling in angiotensin II (Ang II) type 1 (AT₁) transgenic (AT₁Tg)-angiotensinogen-knockout (AgtKO) mice by candesartan but not by candesartan-7H. **A**, Blood pressure–lowering effects of candesartan cilexetil (Can) and candesartan-7H (Can-7H) in Ang II-infused mice. Eight-week-old C57BL/6J male mice were continuously infused with Ang II (0.6 mg/kg per day) and treated with candesartan cilexetil (1 mg/kg per day), candesartan-7H (1, 10, and 20 mg/kg per day), or vehicle in drinking water (n=5, in each group). **P*<0.05, ***P*<0.01 vs vehicle-treated group. **B**, Heart:body weight ratios and gross hearts in AgtKO and AT₁Tg-Agt KO mice (20 weeks of age) treated with Can (1 mg/kg per day), Can-7H (1, 20 mg/kg per day), or vehicle. Data are presented as mean±SEM. Number of mice for each experiment is indicated in the bars. ***P*<0.01. Scale bars, 5 mm. **C**, Left ventricular end-diastolic dimension (LVDD) and fractional shortening (FS) of AT₁Tg-AgtKO mice treated with Can or Can-7H. Can (1 mg/kg per day, n=11), Can-7H (1, 20 mg/kg per day; n=7 in each group), or vehicle (n=7) was given for 14 weeks in 6-week-old AT₁Tg-AgtKO mice. Data are presented as mean±SEM. **P*<0.05, ***P*<0.01 vs vehicle-treated group. **D**, Histological sections with Masson trichrome staining in AgtKO and AT₁Tg-Agt KO mice (20 weeks of age) treated with Can (1 mg/kg per day), Can-7H (1, 20 mg/kg per day), or vehicle. Scale bars, 50 μm. **E**, The mRNA expressions of cardiac genes *Nppa*, *Nppb*, and *Acta1* and extracellular matrix genes *Col3a1* and *Postn* in AgtKO (lane 1) and AT₁Tg-Agt KO mice (20 weeks of age) treated with Can (1 mg/kg per day; lane 3), Can-7H (1, 20 mg/kg per day; lane 4, 5, respectively), or vehicle (lane 2). Data are presented as mean±SEM. ***P*<0.01 vs AgtKO mice. NS indicates not significant (*P*>0.05). □, vehicle; ×, Can-7H (1 mg/kg per d); ▲, Can-7H (10 mg/kg per d); ●, Can-7H (20 mg/kg per d); ◆, Can (1 mg/kg per d).

contribution of endogenous Ang II to the activity of AT₁ receptor in native tissues, we used AgtKO mice, deficient in the production of Ang II.¹³ Furthermore, AT₁Tg-AgtKO mice developed cardiac remodeling regardless of whether they were the offspring of Agt^{+/-} females or Agt^{-/-} females (Figure S3), suggesting that maternal or placental angiotensinogen had little influence on the postnatal development of cardiac remodeling in AT₁Tg-AgtKO mice. Among the renin-angiotensin system components, the mRNA level of the AT₂ receptor was significantly upregulated in AT₁Tg-AgtKO hearts compared with AgtKO hearts (Figure S1A), but the protein level of the AT₂ receptor was comparable between AT₁Tg-AgtKO and AgtKO hearts. Therefore, we believe that constitutive activity of the AT₁ receptor is sufficient for inducing structural and functional cardiac remodeling, when the AT₁ receptor is upregulated in the hearts.

Redistribution of G α_{q11} into the cytosolic fraction in AT₁Tg-AgtKO hearts (Figure 1A) indicates that constitutive activity of the AT₁ receptor is mediated through the G α_{q11} -dependent signaling pathway. On binding to Ang II, the AT₁ receptor is phosphorylated by GPCR kinases and recruits β -arrestins, leading to clathrin-coated, pit-dependent internalization and then recycling to the plasma membrane.²³ It has been reported that constitutively active mutant AT₁ receptors are constitutively internalized and recycled when overexpressed in HEK293 cells.²⁴ In contrast, we showed previously, by immunofluorescence analysis, that the wild-type AT₁ receptor was predominantly localized in the plasma membrane of HEK293 cells expressing the AT₁ receptor.¹ In addition, the expression levels of GPCR kinase 2 and β -arrestins in the particulate fraction relative to the cytosolic fraction were comparable between AT₁Tg-AgtKO and AgtKO hearts (Figure S4). Therefore, we suppose that, in the absence of Ang II, wild-type AT₁ receptor stochastically undergoes subtle and transient conformational changes, leading to partial activation of G α_{q11} -dependent signaling without inducing detectable receptor internalization. The AT₁ receptor can also stimulate G protein-independent diverse signaling pathways involving β -arrestins, tyrosine kinases, reactive oxygen species, and AT₁ receptor-associated proteins.¹⁵ Further structure-function analysis will be needed to elucidate the full breadth of the molecular mechanisms and signal transduction network that mediate agonist-independent AT₁ receptor activation in the hearts.

It has been reported that the AT₁ receptor is upregulated in stressed hearts of spontaneously hypertensive rats,²⁵ 2-kidney 1-clip renovascular hypertensive rats,²⁵ Tsukuba hypertensive mice,²⁶ and rats with myocardial infarction.²⁷ Furthermore, we observed that cardiac expression of the AT₁ receptor was increased \approx 8-fold in pressure-overloaded mice after transverse aortic constriction (B_{\max} : 142.9 \pm 36.5 fmol/mg; n=3) compared with sham-operated mice (B_{\max} : 16.4 \pm 4.9 fmol/mg; n=3). In addition, it has been reported that the AT₁ receptor is upregulated in response to low-density lipoprotein cholesterol,²⁸ insulin,²⁹ glucose,³⁰ progesterone,³¹ and inflammatory cytokines, such as interleukin 1 α or interleukin 6,^{32,33} in vascular cells. Therefore, it seems quite reasonable to assume that enhancement of constitutive activity of the AT₁ receptor through upregulation of receptor expression may accelerate the

progression of atherosclerosis in patients with hypercholesterolemia or diabetes mellitus, especially after menopause. Further studies in animal models will be required to clarify the roles of constitutive activity of the AT₁ receptor in the pathogenesis of cardiovascular and metabolic disorders.

We also demonstrate that treatment with candesartan, inverse agonist for the AT₁ receptor, effectively prevents cardiac remodeling in AT₁Tg-AgtKO mice. The inverse agonist activity of ARBs may provide clinical advantage of inhibiting both Ang II-dependent and -independent receptor activation and, thus, be an important pharmacological parameter defining the beneficial effects on organ protection.³ Several ARBs are currently available for the treatment of hypertension and heart failure with reduced left ventricular ejection fraction, and their potency of inverse agonist activity differs according to the distinct chemical structure of the drug.³ For example, the inhibitory effect of olmesartan on both constitutive activity and stretch-induced activation of the AT₁ receptor was significantly higher than that of losartan.² According to a recent article,³⁴ the use of candesartan was associated with lower all-cause mortality than the use with losartan in a Swedish registry of patients with heart failure. Although EXP3174, an active metabolite of losartan, can act as an inverse agonist,⁸ it is tempting to speculate that the potent inverse agonist activity of candesartan may explain some of its association with lower mortality in patients with heart failure.

Perspectives

Blockade of the renin-angiotensin system has been shown to be beneficial in patients with hypertension, especially those with cardiovascular and metabolic complications. Our findings show that constitutive activity of the AT₁ receptor contributes to the progression of cardiac remodeling even in the absence of Ang II, when the AT₁ receptor is upregulated in the heart. Inverse agonism of ARBs provides therapeutic effects in the prevention of cardiac remodeling induced by constitutive activity of AT₁ receptor and, thus, has potential impact on long-term outcomes in patients with hypertension. Our work is the first proof-of-principle experiment, to our knowledge, on the in vivo importance of constitutive activity of a native GPCR in the pathogenesis of diseases. Beyond in vitro pharmacological tools, inverse agonists emerge as promising pharmacological candidates in treating diseases caused by enhancement of constitutive activity through upregulation of GPCRs.

Acknowledgments

We thank Drs Sin-ichiro Miura (Fukuoka University) and Motohiro Nishida (Kyushu University) for technical advice and Akane Furuyama, Megumi Ikeda, Yuko Ohtsuki, and Ikuko Sakamoto for their excellent technical assistance.

Sources of Funding

This work was supported in part by grants from Japan Society for the Promotion of Science (KAKENHI 20390218, 21229010, and 23390213; to I.K. and H.A.), Health and Labor Sciences Research grants, Kowa Life Science Foundation, Takeda Science Foundation, Astellas Foundation for Research on Metabolic Disorders, the Uehara Memorial Foundation, the Ichiro Kanehara Foundation,

Mochida Memorial Foundation for Medical and Pharmaceutical Research, and Suzuken Memorial Foundation (to H.A.).

Disclosures

None.

References

- Yasuda N, Miura S, Akazawa H, Tanaka T, Qin Y, Kiya Y, Imaizumi S, Fujino M, Ito K, Zou Y, Fukuhara S, Kunimoto S, Fukuzaki K, Sato T, Ge J, Mochizuki N, Nakaya H, Saku K, Komuro I. Conformational switch of angiotensin II type 1 receptor underlying mechanical stress-induced activation. *EMBO Rep*. 2008;9:179–186.
- Qin Y, Yasuda N, Akazawa H, Ito K, Kudo Y, Liao CH, Yamamoto R, Miura S, Saku K, Komuro I. Multivalent ligand-receptor interactions elicit inverse agonist activity of AT(1) receptor blockers against stretch-induced AT(1) receptor activation. *Hypertens Res*. 2009;32:875–883.
- Akazawa H, Yasuda N, Komuro I. Mechanisms and functions of agonist-independent activation in the angiotensin II type 1 receptor. *Mol Cell Endocrinol*. 2009;302:140–147.
- Milligan G. Constitutive activity and inverse agonists of G protein-coupled receptors: a current perspective. *Mol Pharmacol*. 2003;64:1271–1276.
- Zou Y, Akazawa H, Qin Y, Sano M, Takano H, Minamino T, Makita N, Iwanaga K, Zhu W, Kudoh S, Toko H, Tamura K, Kihara M, Nagai T, Fukamizu A, Umemura S, Iiri T, Fujita T, Komuro I. Mechanical stress activates angiotensin II type 1 receptor without the involvement of angiotensin II. *Nat Cell Biol*. 2004;6:499–506.
- Mederos Y, Schnitzler M, Storch U, Meibers S, Nurwakagari P, Breit A, Essin K, Gollasch M, Gudermann T. Gq-coupled receptors as mechanosensors mediating myogenic vasoconstriction. *EMBO J*. 2008;27:3092–3103.
- Rakesh K, Yoo B, Kim IM, Salazar N, Kim KS, Rockman HA. β -Arrestin-biased agonism of the angiotensin receptor induced by mechanical stress. *Sci Signal*. 2010;3:ra46.
- Miura S, Fujino M, Hanzawa H, Kiya Y, Imaizumi S, Matsuo Y, Tomita S, Uehara Y, Karnik SS, Yanagisawa H, Koike H, Komuro I, Saku K. Molecular mechanism underlying inverse agonist of angiotensin II type 1 receptor. *J Biol Chem*. 2006;281:19288–19295.
- Sachse R, Shao XJ, Rico A, Finckh U, Rolfs A, Reincke M, Hensen J. Absence of angiotensin II type 1 receptor gene mutations in human adrenal tumors. *Eur J Endocrinol*. 1997;137:262–266.
- Davies E, Bonnardeaux A, Plouin PF, Corvol P, Clauser E. Somatic mutations of the angiotensin II (AT1) receptor gene are not present in aldosterone-producing adenoma. *J Clin Endocrinol Metab*. 1997;82:611–615.
- Billet S, Bardin S, Verp S, Baudrie V, Michaud A, Conchon S, Muffat-Joly M, Escoubet B, Souil E, Hamard G, Bernstein KE, Gasc JM, Elghozi JL, Corvol P, Clauser E. Gain-of-function mutant of angiotensin II receptor, type 1A, causes hypertension and cardiovascular fibrosis in mice. *J Clin Invest*. 2007;117:1914–1925.
- Paradis P, Dali-Youcef N, Paradis FW, Thibault G, Nemer M. Overexpression of angiotensin II type I receptor in cardiomyocytes induces cardiac hypertrophy and remodeling. *Proc Natl Acad Sci USA*. 2000;97:931–936.
- Tanimoto K, Sugiyama F, Goto Y, Ishida J, Takimoto E, Yagami K, Fukamizu A, Murakami K. Angiotensinogen-deficient mice with hypotension. *J Biol Chem*. 1994;269:31334–31337.
- Miura S, Feng YH, Husain A, Karnik SS. Role of aromaticity of agonist switches of angiotensin II in the activation of the AT1 receptor. *J Biol Chem*. 1999;274:7103–7110.
- Hunyady L, Catt KJ. Pleiotropic AT1 receptor signaling pathways mediating physiological and pathogenic actions of angiotensin II. *Mol Endocrinol*. 2006;20:953–970.
- Zhai P, Galeotti J, Liu J, Holle E, Yu X, Wagner T, Sadoshima J. An angiotensin II type 1 receptor mutant lacking epidermal growth factor receptor transactivation does not induce angiotensin II-mediated cardiac hypertrophy. *Circ Res*. 2006;99:528–536.
- Shibouta Y, Inada Y, Ojima M, Wada T, Noda M, Sanada T, Kubo K, Kohara Y, Naka T, Nishikawa K. Pharmacological profile of a highly potent and long-acting angiotensin II receptor antagonist, 2-ethoxy-1-[[2'-(1H-tetrazol-5-yl)biphenyl-4-yl]methyl]-1H-benzimidazole-7-carboxylic acid (CV-11974), and its prodrug, (+/-)-1-(cyclohexyloxycarbonyloxy)-ethyl 2-ethoxy-1-[[2'-(1H-tetrazol-5-yl)biphenyl-4-yl]methyl]-1H-benzimidazole-7-carboxylate (TCV-116). *J Pharmacol Exp Ther*. 1993;266:114–120.
- Morrisset S, Rouleau A, Ligneau X, Gbahou F, Tardivel-Lacombe J, Stark H, Schunack W, Ganellin CR, Schwartz JC, Arrang JM. High constitutive activity of native H3 receptors regulates histamine neurons in brain. *Nature*. 2000;408:860–864.
- Srinivasan S, Lubrano-Berthelie C, Govaerts C, Picard F, Santiago P, Conklin BR, Vaisse C. Constitutive activity of the melanocortin-4 receptor is maintained by its N-terminal domain and plays a role in energy homeostasis in humans. *J Clin Invest*. 2004;114:1158–1164.
- Pantel J, Legendre M, Cabrol S, Hilal L, Hajaji Y, Morisset S, Nivot S, Vie-Luton MP, Grouselle D, de Kerdanet M, Kadiri A, Epelbaum J, Le Bouc Y, Amselem S. Loss of constitutive activity of the growth hormone secretagogue receptor in familial short stature. *J Clin Invest*. 2006;116:760–768.
- Parma J, Duprez L, Van Sande J, Cochaux P, Gervy C, Mockel J, Dumont J, Vassart G. Somatic mutations in the thyrotropin receptor gene cause hyperfunctioning thyroid adenomas. *Nature*. 1993;365:649–651.
- Shenker A, Laue L, Kosugi S, Merendino JJ Jr, Minegishi T, Cutler GB Jr. A constitutively activating mutation of the luteinizing hormone receptor in familial male precocious puberty. *Nature*. 1993;365:652–654.
- Shenoy SK, Lefkowitz RJ. Angiotensin II-stimulated signaling through G proteins and β -arrestin. *Sci STKE*. 2005;2005:cm14.
- Miserey-Lenkei S, Parnot C, Bardin S, Corvol P, Clauser E. Constitutive internalization of constitutively active angiotensin II AT(1A) receptor mutants is blocked by inverse agonists. *J Biol Chem*. 2002;277:5891–5901.
- Suzuki J, Matsubara H, Urakami M, Inada M. Rat angiotensin II (type 1A) receptor mRNA regulation and subtype expression in myocardial growth and hypertrophy. *Circ Res*. 1993;73:439–447.
- Fujii N, Tanaka M, Ohnishi J, Yukawa K, Takimoto E, Shimada S, Naruse M, Sugiyama F, Yagami K, Murakami K, Miyazaki H. Alterations of angiotensin II receptor contents in hypertrophied hearts. *Biochem Biophys Res Commun*. 1995;212:326–333.
- Nio Y, Matsubara H, Murasawa S, Kanasaki M, Inada M. Regulation of gene transcription of angiotensin II receptor subtypes in myocardial infarction. *J Clin Invest*. 1995;95:46–54.
- Nickenig G, Jung O, Strehlow K, Zolk O, Linz W, Scholkens BA, Bohm M. Hypercholesterolemia is associated with enhanced angiotensin AT1-receptor expression. *Am J Physiol*. 1997;272:H2701–H2707.
- Nickenig G, Røling J, Strehlow K, Schnabel P, Bohm M. Insulin induces upregulation of vascular AT1 receptor gene expression by posttranscriptional mechanisms. *Circulation*. 1998;98:2453–2460.
- Sodhi CP, Kanwar YS, Sahai A. Hypoxia and high glucose upregulate AT1 receptor expression and potentiate ANG II-induced proliferation in VSM cells. *Am J Physiol Heart Circ Physiol*. 2003;284:H846–H852.
- Nickenig G, Strehlow K, Wassmann S, Baumer AT, Albory K, Sauer H, Bohm M. Differential effects of estrogen and progesterone on AT(1) receptor gene expression in vascular smooth muscle cells. *Circulation*. 2000;102:1828–1833.
- Wassmann S, Stumpf M, Strehlow K, Schmid A, Schieffer B, Bohm M, Nickenig G. Interleukin-6 induces oxidative stress and endothelial dysfunction by overexpression of the angiotensin II type 1 receptor. *Circ Res*. 2004;94:534–541.
- Sasamura H, Nakazato Y, Hayashida T, Kitamura Y, Hayashi M, Saruta T. Regulation of vascular type 1 angiotensin receptors by cytokines. *Hypertension*. 1997;30:35–41.
- Eklind-Cervenka M, Benson L, Dahlstrom U, Edner M, Rosenqvist M, Lund LH. Association of candesartan vs losartan with all-cause mortality in patients with heart failure. *JAMA*. 2011;305:175–182.

ONLINE SUPPLEMENT

AGONIST-INDEPENDENT CONSTITUTIVE ACTIVITY OF ANGIOTENSIN II RECEPTOR PROMOTES CARDIAC REMODELING IN MICE

Noritaka Yasuda¹, Hiroshi Akazawa², Kaoru Ito¹, Ippei Shimizu¹, Yoko Kudo-Sakamoto², Chizuru Yabumoto², Masamichi Yano², Rie Yamamoto¹, Yukako Ozasa¹, Tohru Minamino¹, Atsuhiko T. Naito³, Toru Oka², Ichiro Shiojima³, Kouichi Tamura⁴, Satoshi Umemura⁴, Mona Nemer⁵, Issei Komuro²

1. Department of Cardiovascular Science and Medicine, Chiba University Graduate School of Medicine, 1-8-1 Inohana, Chuo-ku, Chiba 260-8670, Japan.
2. Department of Cardiovascular Medicine,
3. Department of Cardiovascular Regenerative Medicine, Osaka University Graduate School of Medicine, 2-2 Yamadaoka, Suita, Osaka 565-0871, Japan
4. Department of Medical Science and Cardiorenal Medicine, Yokohama City University Graduate School of Medicine, 3-9 Fukuura, Kanazawa-ku, Yokohama 236-0004, Japan
5. Laboratory of Cardiac Growth and Differentiation, Department of Biochemistry, Microbiology and Immunology, Faculty of Medicine, University of Ottawa, 550 Cumberland, Ottawa, Ontario K1N 6N5, Canada

Correspondence to:

Issei Komuro, M.D., Ph.D.

Department of Cardiovascular Medicine,
Osaka University Graduate School of Medicine,
2-2 Yamadaoka, Suita, Osaka 565-0871, Japan.
TEL: +81-6-6879-3631
FAX: +81-6-6879-3639
E-mail: komuro-ty@umin.ac.jp

Supplemental Materials and Methods

Mice, TAC operation, and transthoracic echocardiography

Mice expressing the human *AGTR1a* gene under the control of α -myosin heavy chain (*MHC*) promoter and mice deficient for *Agt* gene were previously described^{1,2}. We crossed *AGTR1a*^{Tg/o} mice (on the C57BL/6 background) with *Agt*^{-/-} mice (on the ICR background), and then bred the resulting *AGTR1a*^{Tg/o}/*Agt*^{+/-} offspring with *Agt*^{+/-} mice to generate *AGTR1a*^{Tg/o}/*Agt*^{+/+} (AT₁Tg), *AGTR1a*^{Tg/o}/*Agt*^{-/-} (AT₁Tg-AgtKO), and *AGTR1a*^{o/o}/*Agt*^{-/-} (AgtKO) mice. We also generated *AGTR1a*^{Tg/o}/*Agt*^{-/-} (AT₁Tg-AgtKO) by crossing *AGTR1a*^{Tg/o}/*Agt*^{+/-} with *Agt*^{-/-} mice. C57BL/6 mice were purchased from Japan SLC. Candesartan and candesartan-7H were synthesized in Takeda Pharmaceutical Co., Ltd., and administered via drinking water. For TAC operation, 10-week-old male mice were anesthetized by i.p. injection of pentobarbital (50 mg/kg), and respiration was artificially controlled with a tidal volume of 0.2 ml and a respiratory rate of 110 breaths/min. The transverse aorta was constricted with 7-0 nylon strings by ligating the aorta with splinting a blunted 27 gauge needle, which was removed after the ligation. After aortic constriction, the chest was closed and mice were allowed to recover from anesthesia. We confirmed that the magnitude of initial pressure elevation after aortic banding was identical in all groups of mice. The surgeon had no information about the mice used in this study. For evaluation of cardiac dimensions and contractility, transthoracic echocardiography was performed on conscious mice with Vevo 770 Imaging System using a 25 MHz linear probe (Visual Sonics). All protocols were approved by the Institutional Animal Care and Use Committee of Chiba University.

Ang II infusion and BP measurement

Ang II (Sigma-Aldrich) was dissolved in 0.9% saline. Eight-week-old C57BL/6J male mice were treated with Ang II (0.6 mg/kg/day) or vehicle for 2 weeks using an osmotic mini-pump (ALZET model 2002; Durent Corp.). The systolic and diastolic BP and pulse rates were measured in conscious mice noninvasively by a programmable sphygmomanometer (BP-98A, Softron) using the tail-cuff method.

Real-time RT-PCR analysis

Total RNA was extracted by using RNeasy Kit (Qiagen), and single-stranded cDNA was transcribed by using QuantiTect Reverse Transcription Kit (Qiagen), according to the manufacturer's protocol. We conducted quantitative real-time PCR analysis with the Universal ProbeLibrary Assays (Roche Applied Science), according to the manufacturer's instructions. Amplification conditions were initial denaturation for 10 min at 95°C followed by 45 cycles of 10 s at 95°C and 25 s at 60°C. Individual PCR products were analyzed by melting-point analysis. The expression level of a gene was normalized relative to that of *Gapdh* by using a comparative Ct method. The primer sequences and Universal Probe numbers were designed with the ProbeFinder software as following: *Agtr1b*, 5'-cgccagcagcactgtaga-3' and 5'-ggagggggtgaattcaaaa-3', No. 32; *Agtr2*, 5'-ggagctcggaactgaaagc-3' and 5'-ctgcagcaactccaaattctt-3', No. 41; *Ace*, 5'-tatgccctggaacctgat-3' and 5'-gatggctctccccacctt-3', No. 78; *Ren1*, 5'-ggaggaagtgttctctgtactaca-3' and 5'-tcgctacctctagcaccac-3', No. 3; *Ren2*,

5'-catggagaatggagacgactt-3' and 5'-cacagtgattccaccacag-3', No. 102; *Nppa*, 5'-cacagatctgatggattcaaga-3' and 5'-cctcatcttctaccggcatc-3', No. 25; *Nppb*, 5'-gtcagtcggttgggctgtaac-3' and 5'-agaccaggcagagtcagaa-3', No. 71; *Acta1*, 5'-agctatgagctgcctgacg-3' and 5'-atccccgagactccatac-3', No. 9; *Col3a1*, 5'-tcccctggaatctgtgaatc-3' and 5'-tgagtgcgaattggggagaat-3', No. 49; *Postn*, 5'-cgggaagaacgaatcattaca-3' and 5'-acctggagacctcttttgc-3', No. 10; *Gapdh*, 5'-gtccgctcgtggatctgac-3' and 5'-cctgctcaccaccttcttg-3', No. 80.

Western blot analysis and subcellular fractionation

Protein samples were fractionated with SDS-PAGE, transferred to PVDF membranes (GE Healthcare Biosciences). The blotted membranes were incubated with primary antibody, followed by horseradish peroxidase-conjugated secondary antibody (Jackson ImmunoResearch Laboratories). Immunoreactive signals were visualized using ECL Plus Western Blotting Detection System (GE Healthcare Biosciences). Following antibodies were used: rabbit polyclonal anti-G $\alpha_{q/11}$ antibody, goat polyclonal anti-GAPDH antibody (Santa Cruz Biotechnology, Inc.), rabbit polyclonal anti-phospho-ERK1/2 antibody (Cell Signaling Technology), rabbit polyclonal anti-ERK1/2 antibody (Invitrogen), rabbit polyclonal anti-AT₂ receptor antibody (Alomone Labs), mouse monoclonal anti-GRK2 antibody (Santa Cruz), and mouse monoclonal anti- β -arrestin 1/2 antibody (Santa Cruz).

For subcellular fractionation, heart samples were homogenized in lysis buffer (25 mM Tris HCl pH 7.4, 5 mM EGTA, 2 mM EDTA, 100 mM NaF, 5 mM DTT) plus protease inhibitors (Complete mini; Roche Applied Science). The lysates were centrifuged at 500 g for 20 min to pellet unbroken cells and nuclei. The supernatant was centrifuged at 100,000 g for 60 min, and the supernatant was designated as the cytosolic fraction. The pellets were then resuspended as the membrane-particulate fraction in lysis buffer with 1% Triton X-100.

Histological analysis Hearts were excised, fixed immediately in 10% neutralized formalin, and embedded in paraffin. Serial sections at 5 μ m were stained with Masson's trichrome for evaluation of fibrosis.

Radioligand receptor binding assay Radioligand-binding assays were performed as described previously³⁻⁵. The protein in membrane fraction was incubated with 100 pM ¹²⁵I-[Sar¹, Ile⁸] Ang II (Perkin Elmer) for 1 hr at 22°C. Binding reaction was terminated by filtering the incubation mixture through Whatman GF/C glass filters (GE healthcare Biosciences), and the residues were extensively washed further with binding buffer. The bound ligand fraction was determined from the counts per minute (cpm) remaining on the membrane. Binding kinetics values were determined with the LIGAND computer program (Elsevier-Biosoft), as previously described³⁻⁵.

Statistics

All data are presented as means \pm SEM. Two-group comparison was analyzed by unpaired 2-tailed Student's *t* test, and multiple-group comparison was performed by one-way ANOVA followed by the Fisher's PLSD test for comparison of means. A probability value of *P* < 0.05 was considered to be statistically significant.

References

1. Paradis P, Dali-Youcef N, Paradis FW, Thibault G, Nemer M. Overexpression of angiotensin II type I receptor in cardiomyocytes induces cardiac hypertrophy and remodeling. *Proc Natl Acad Sci U S A*. 2000;97:931-936.
2. Tanimoto K, Sugiyama F, Goto Y, Ishida J, Takimoto E, Yagami K, Fukamizu A, Murakami K. Angiotensinogen-deficient mice with hypotension. *J Biol Chem*. 1994;269:31334-31337.
3. Miura S, Feng YH, Husain A, Karnik SS. Role of aromaticity of agonist switches of angiotensin II in the activation of the AT1 receptor. *J Biol Chem*. 1999;274:7103-7110.
4. Yasuda N, Miura S, Akazawa H, Tanaka T, Qin Y, Kiya Y, Imaizumi S, Fujino M, Ito K, Zou Y, Fukuhara S, Kunimoto S, Fukuzaki K, Sato T, Ge J, Mochizuki N, Nakaya H, Saku K, Komuro I. Conformational switch of angiotensin II type 1 receptor underlying mechanical stress-induced activation. *EMBO Rep*. 2008;9:179-186.
5. Akazawa H, Yasuda N, Miura S, Komuro I. Assessment of inverse agonism for the angiotensin II type 1 receptor. *Methods Enzymol*. 2010;485:25-35.

Figure S1

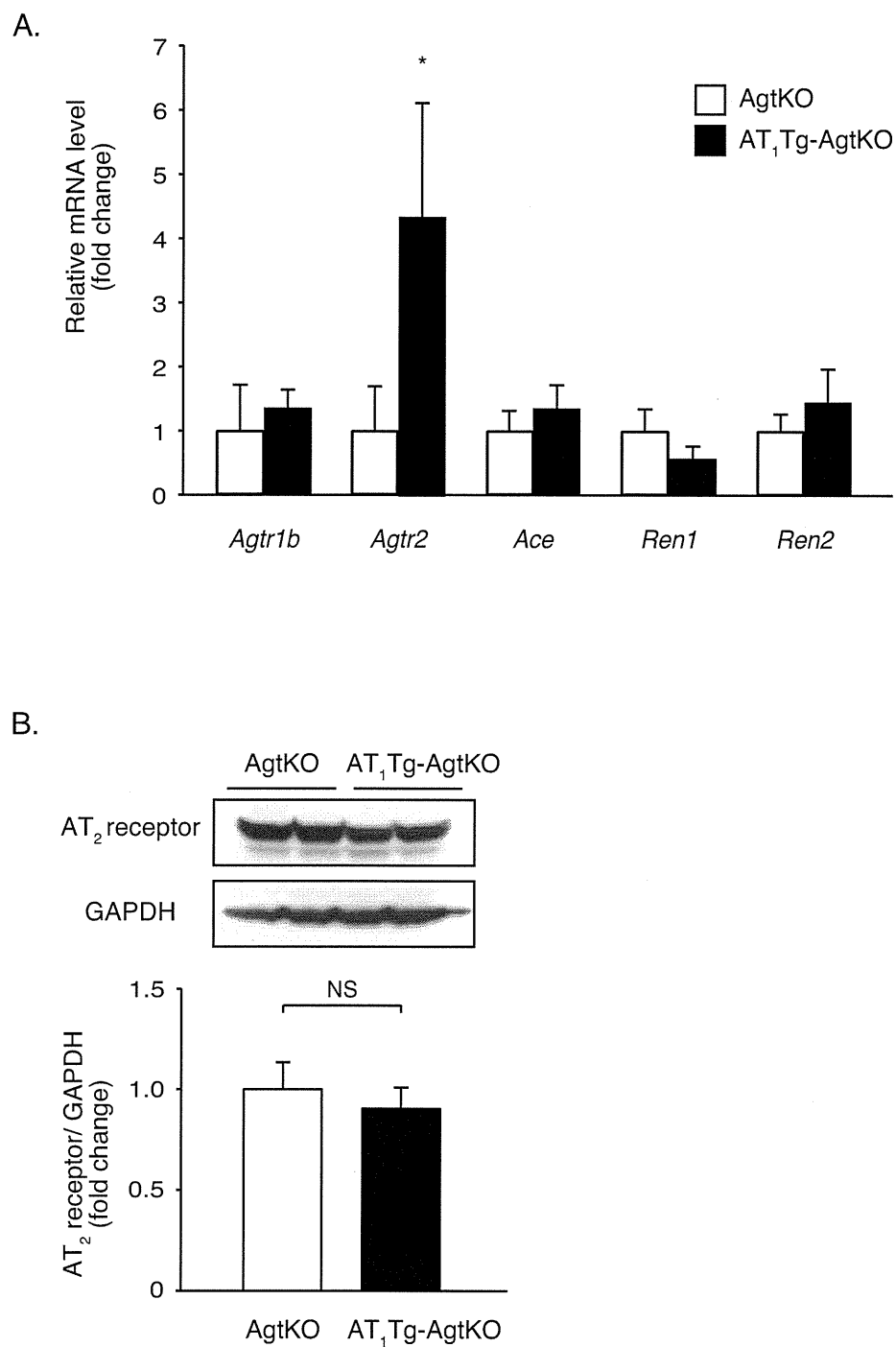


Figure S1. Expression levels of the renin-angiotensin system components in AT₁Tg-Agt KO and AgtKO hearts. (A) The mRNA expressions of the renin-angiotensin system components in AT₁Tg-Agt KO ($n = 6$) and AgtKO hearts ($n = 6$) at 20 weeks of age. Data are presented as mean \pm SEM. * $P < 0.05$ versus AgtKO mice. (B) Immunoblot analysis of AT₂ receptor in AgtKO ($n = 4$) and AT₁Tg-AgtKO ($n = 4$) hearts at 20 weeks of age. GAPDH was used as an internal control for loading. The quantitation of the AT₂ receptor /GAPDH is shown as a bar graph. Data are presented as mean \pm SEM. NS, not significant ($P > 0.05$).

Figure S2

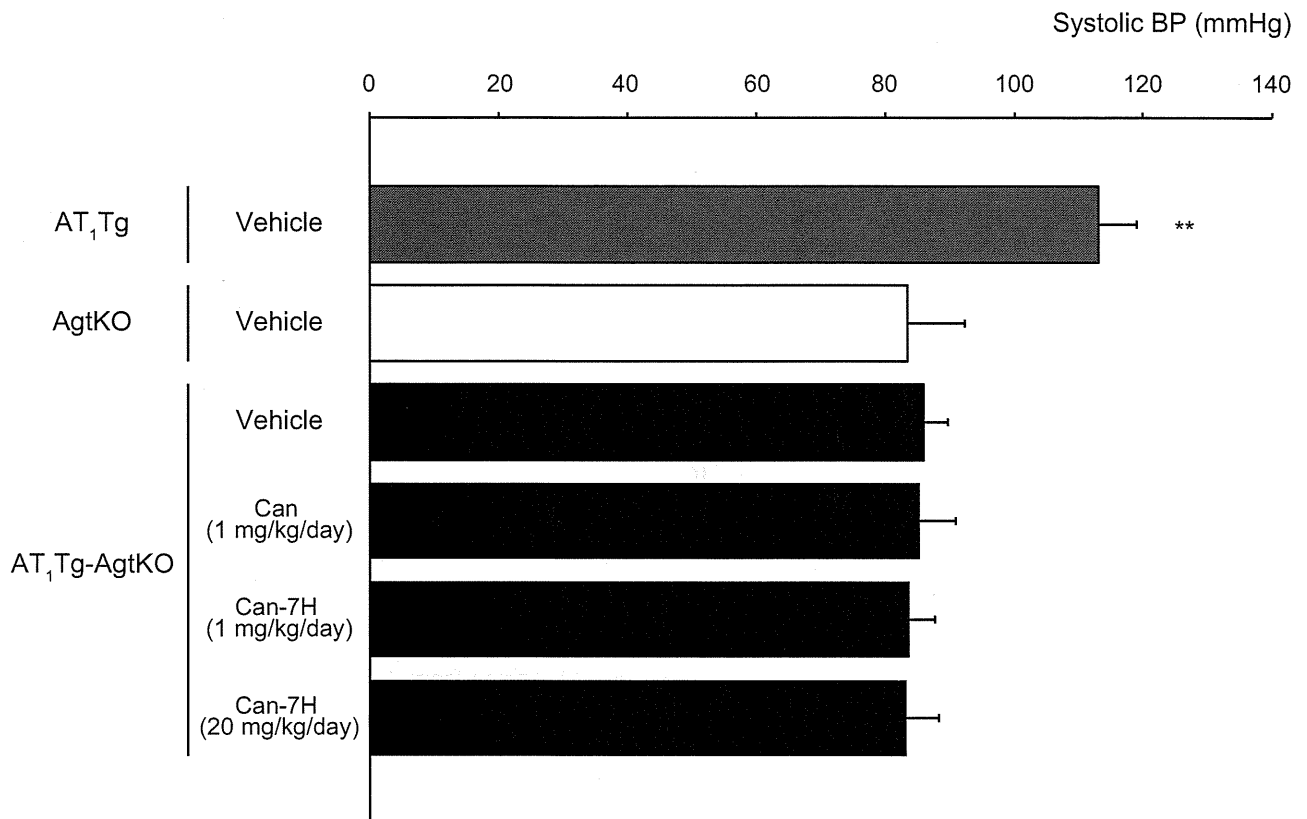


Figure S2. Systolic BP in AT₁Tg mice treated with vehicle ($n = 9$), AgtKO mice treated with vehicle ($n = 6$), AT₁Tg-AgtKO mice treated with vehicle ($n = 6$), candesartan cilexetil (Can) (1 mg/kg/day, $n = 8$) or candesartan-7H (Can-7H) (1 mg/kg/day, $n = 5$ or 20 mg/kg/day, $n = 5$). BP was measured in 20-week-old mice after the treatment for 14 weeks. Data are presented as mean \pm SEM. ** $P < 0.01$ versus AgtKO mice.

Figure S3

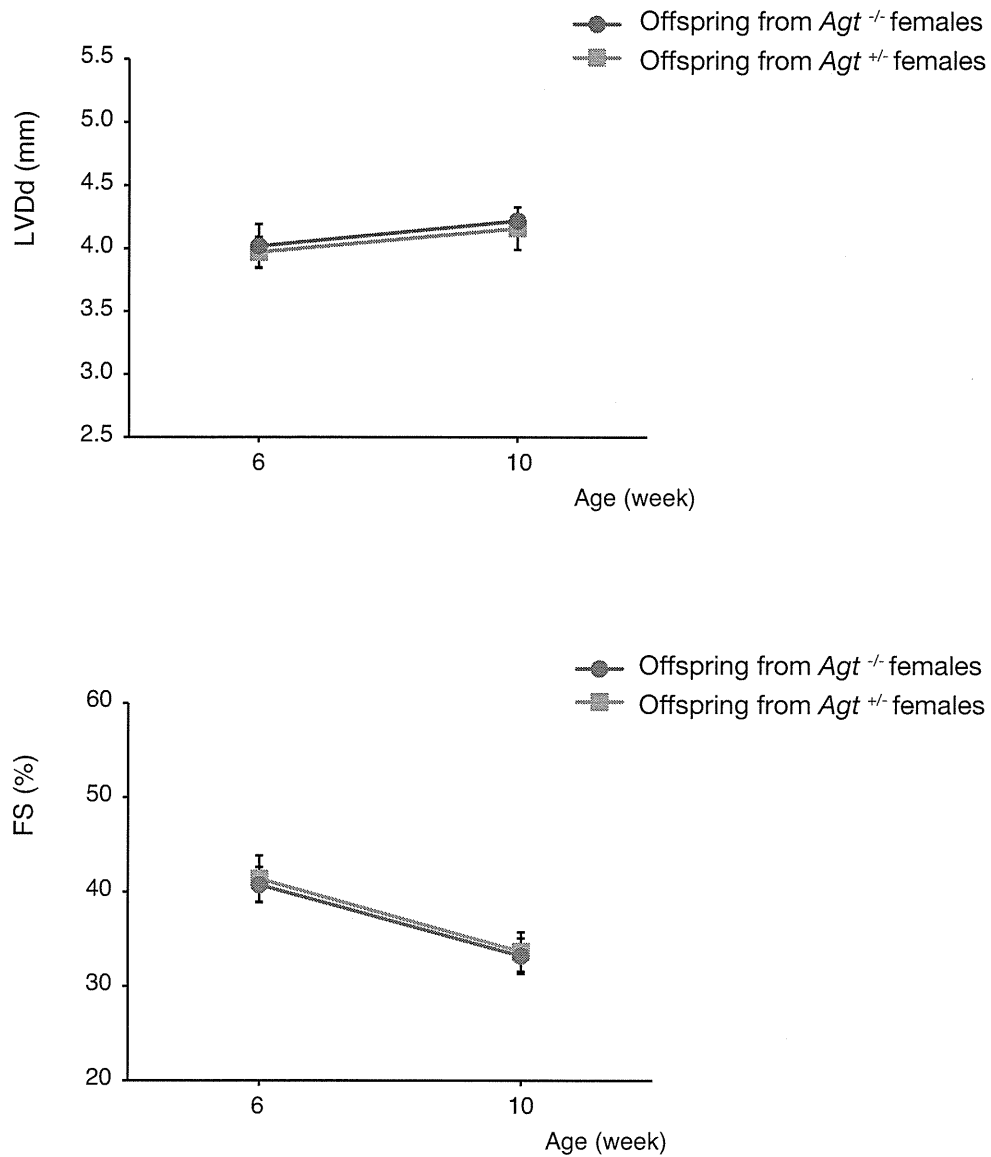


Figure S3. AT₁Tg-AgtKO mice developed cardiac remodeling independently of the effects of maternal or placental angiotensinogen during the fetal period. Left ventricular end-diastolic dimension (LVDd) and fractional shortening (FS) of AT₁Tg-AgtKO offspring of *Agt*^{+/-} females ($n = 4$) or *Agt*^{-/-} females ($n = 4$), measured by echocardiogram at 6 and 10 weeks of age. Data are presented as mean \pm SEM.

Figure S4

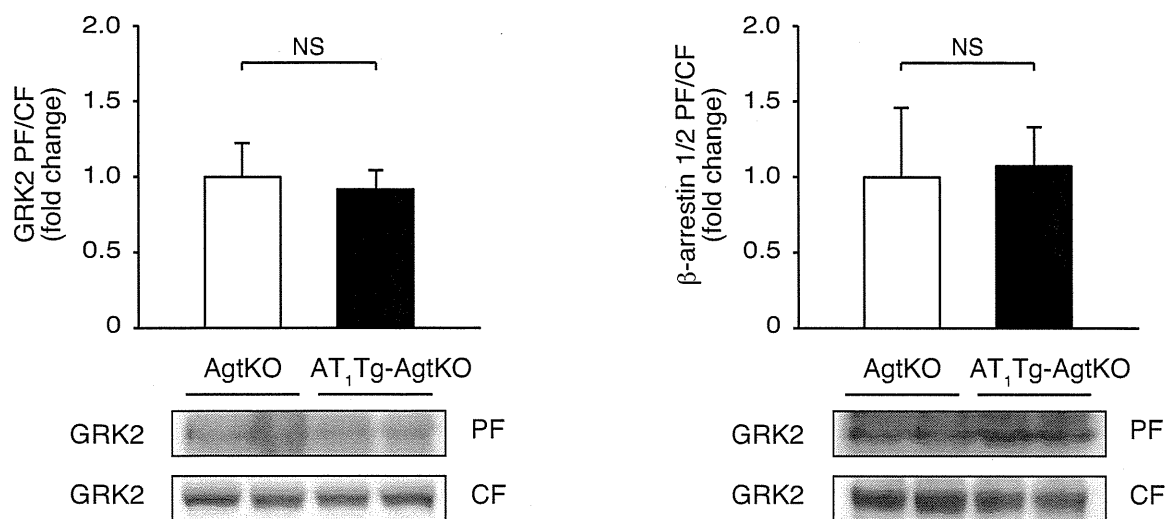
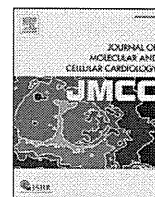


Figure S4. Immunoblot analysis of GRK2 and β-arrestin 1/2 in particulate fraction (PF) and cytosolic fraction (CF) extracted from AgtKO ($n = 4$) and AT₁Tg-Agt KO ($n = 4$) hearts. The quantitation of GRK2 in PF/CF and β-arrestin 1/2 in PF/CF is shown as bar graphs. Data are presented as mean \pm SEM. NS, not significant ($P > 0.05$).



Contents lists available at SciVerse ScienceDirect

Journal of Molecular and Cellular Cardiology

journal homepage: www.elsevier.com/locate/yjmcc

Original article

Role of regulatory T cells in atheroprotective effects of granulocyte colony-stimulating factor

Raita Uchiyama^{a,1}, Hiroshi Hasegawa^{a,1}, Yoshihito Kameda^a, Kazutaka Ueda^a, Yoshio Kobayashi^a, Issei Komuro^b, Hiroyuki Takano^{c,*}^a Department of Cardiovascular Science and Medicine, Chiba University Graduate School of Medicine, 1-8-1 Inohana, Chuo-ku, Chiba 260-8670, Japan^b Department of Cardiovascular Medicine, Osaka University Graduate School of Medicine, 2-2 Yamadaoka, Suita, Osaka 565-0871, Japan^c Department of Molecular Cardiovascular Pharmacology, Chiba University Graduate School of Pharmaceutical Sciences, 1-8-1 Inohana, Chuo-ku, Chiba 260-8675, Japan

ARTICLE INFO

Article history:

Received 9 September 2011

Received in revised form 7 December 2011

Accepted 29 December 2011

Available online xxx

Keywords:

Atherosclerosis
Regulatory T cells
G-CSF
Cytokine
Foxp3

ABSTRACT

We and others have previously reported that granulocyte colony-stimulating factor (G-CSF) prevents left ventricular remodeling and dysfunction after myocardial infarction in animal models and human. We have also reported that G-CSF inhibits the progression of atherosclerosis in animal models, but its precise mechanism is still elusive. So, we examined the effects of G-CSF on atherosclerosis in apolipoprotein E-deficient (ApoE^{-/-}) mice. Twelve-week-old male ApoE^{-/-} mice were subcutaneously administered with 200 µg/kg of G-CSF or saline once a day for 5 consecutive days per a week for 4 weeks. Atherosclerotic lesion of aortic sinus was significantly reduced in the G-CSF-treated mice compared with the saline-treated mice (35% reduction, $P < 0.05$). G-CSF significantly reduced the expression level of interferon- γ by 31% and increased the expression level of interleukin-10 by 20% in atherosclerotic lesions of aortic sinus. G-CSF increased the number of CD4⁺CD25⁺ regulatory T cells in lymph nodes and spleen, and enhanced the suppressive function of regulatory T cells *in vitro*. G-CSF markedly increased the number of Foxp3-positive regulatory T cells in atherosclerotic lesions of aortic sinus. Administration of anti-CD25 antibody (PC61) that depletes regulatory T cells abrogated these atheroprotective effects of G-CSF. Moreover, in ApoE^{-/-}/CD28^{-/-} mice, that lack regulatory T cells, the protective effects of G-CSF on atherosclerosis were not recognized. These findings suggest that regulatory T cells play an important role in the atheroprotective effects of G-CSF.

© 2012 Elsevier Ltd. All rights reserved.

1. Introduction

Atherosclerosis is a progressive disease characterized by the accumulation of lipids and fibrous elements in arterial walls. Over the past two decades, an understanding of the importance of inflammation in the initiation and progression of atherosclerosis has greatly increased. Under normal conditions, the endothelial cells of the arterial wall resist adhesion and aggregation of leukocytes and promote fibrinolysis. When activated by stimuli such as hypertension, smoking, insulin resistance or inflammation, the endothelial cells express a series of adhesion molecules that selectively recruit various classes of leukocytes. Blood monocytes, which are the most numerous inflammatory cells within the atherosclerotic lesions, adhere to the dysfunctional endothelial surface by binding to leukocyte adhesion molecules [1]. Helper T cells and the associated cytokines have been reported to play a crucial role in the pathophysiology of atherosclerosis. CD4⁺CD25⁺ regulatory T cells

(Tregs) subset constitutes 5–10% of all peripheral CD4⁺ T cell population and are specialized for the suppressions of both type 1 helper T (Th1) and type 2 helper T (Th2) immune responses [2]. Tregs, as dedicated suppressors of diverse immune responses and important gatekeepers of immune homeostasis, contribute to the maintenance of the peripheral tolerance. Recently, it was reported that Tregs prevent the progression of atherosclerosis and a defect in Tregs favors atherogenesis [3–5].

Granulocyte colony-stimulating factor (G-CSF) is a member of a group of glycoproteins called hematopoietic cytokines. G-CSF induces the release of hematopoietic stem cells and endothelial progenitor cells from bone marrow into the peripheral blood circulation [6]. Moreover, G-CSF has been reported to modulate immune system and ameliorate immune-mediated diseases of animals [7]. We and others have previously reported that G-CSF prevents left ventricular remodeling and dysfunction after myocardial infarction (MI) in animal models and human [8–12]. G-CSF activates multiple signaling pathways such as Akt and Janus family kinase-2 and signal transducer and activation of transcription-3 (Jak2-STAT3) pathway in cardiac myocytes. G-CSF decreases cardiomyocyte death and increases the number of blood vessels, suggesting the importance of direct actions of G-CSF on the myocardium rather than through mobilization and differentiation of

* Corresponding author at: Department of Molecular Cardiovascular Pharmacology, Chiba University Graduate School of Pharmaceutical Sciences, 1-8-1 Inohana, Chuo-ku, Chiba 260-8675, Japan. Tel./fax: +81 43 226 2883

E-mail address: htakano-cib@umin.ac.jp (H. Takano).

¹ These authors contributed equally to this work.

stem cells. We and others also reported that G-CSF prevents the progression of atherosclerosis [13–16]. G-CSF significantly reduced the stenosis score of coronary artery and lipid plaque area of thoracic aorta in the myocardial infarction-prone Watanabe heritable hyperlipidemic (WHHL-MI) rabbits and prevented an increase in neointima/media ratio in the vascular injury model of rabbit [13]. However, its precise mechanism of G-CSF on atherosclerosis has been still elusive. In human and animal studies, G-CSF stimulation alters the T cell function and modulates the balance between Th1 and Th2 immune responses by affecting cytokine production [17]. G-CSF stimulation reduces cytotoxic activity and proliferative response of human and murine T cells [18]. Recently, G-CSF was reported to prevent autoimmune type 1 diabetes, graft-versus-host disease and transplanted heart allograft acceptability through enhancement of CD4⁺CD25⁺ Tregs subset [19,20]. Therefore, the aim of this study was to elucidate whether Tregs subset is involved in the atheroprotective mechanism of G-CSF.

2. Materials and methods

2.1. Animal model of atherosclerosis

Apolipoprotein E-deficient (ApoE^{-/-}) mice were purchased from the Jackson Laboratory (Bar Harbor, ME). Twelve-week-old male ApoE^{-/-} mice were fed with a proatherogenic diet (1.25% cholesterol, 7.5% cocoa butter, 7.5% casein, 0.5% sodium cholate) (Oriental Yeast Co., Tokyo, Japan) ad libitum for 28 days [21]. These animals were then divided into 2 groups: saline group that received saline and G-CSF group that received G-CSF (rhG-CSF, Kirin Brewery Co., Ltd., Tokyo, Japan). Mice were subcutaneously administrated with 200 µg/kg of G-CSF or same volume (100 µl) of saline once a day for 5 consecutive days per a week for 4 weeks. After 28 days of G-CSF or saline treatment, mice were sacrificed and analyzed.

To deplete Tregs, twelve-week-old male ApoE^{-/-} mice were intraperitoneally injected 100 µg of purified anti-mouse CD25 antibody (clone PC61; Biolegend, San Diego, CA) at day 0 and day 14. These Tregs-depleted mice started proatherogenic diet and each treatment from day 0. At 28 days after first injection, mice were sacrificed and analyzed. To determine the role of Tregs in the mechanisms of G-CSF-induced atheroprotective effect, we used CD28^{-/-} mice. The construction and characterization of CD28^{-/-} mice has been described previously [22]. ApoE^{-/-} mice were crossed with CD28^{-/-} mice and the heterozygous progeny were intercrossed to generate ApoE^{-/-}/CD28^{-/-} double knockout (DKO) mice. Animal genotype was identified by a polymerase chain reaction (PCR)-based assay. All protocols were approved by the Institutional Animal Care and Use Committee of Chiba University.

2.2. Atherosclerotic lesion assessment at aortic sinus

After overnight fasting, blood was collected by the cardiac puncture under anesthetic condition using pentobarbital sodium (60 mg/kg intraperitoneal injection). Serum total cholesterol and high-density

lipoprotein cholesterol levels were determined by high-performance liquid chromatography at SRL (Tokyo, Japan).

The aorta was perfused *in situ* with phosphate buffered saline (PBS), and the heart was removed and the proximal aorta containing the aortic sinus was embedded in OCT compounds (Tissue-Tek, CA). Five sections (10 µm thickness) of the aortic sinus were collected from each mouse and stained with Oil Red-O (Sigma-Aldrich, St Louis, MO) as described previously [21]. For the quantitative analysis of the area of atherosclerosis, section images were captured digitally (Axio Vision, Zeiss, Germany) and the average lesion areas of five separate sections from each mouse were obtained with Image J 1.38 (National Institutes of Health, MD).

2.3. Immunohistochemistry

Immunohistochemical staining with CD3ε (Santa Cruz Biotechnology, Santa Cruz, CA), MOMA-2 (BMA Biomedicals AG, Switzerland), IFN-γ (Biosource International, Camarillo, CA), interleukin-10 (IL-10) (Santa Cruz Biotechnology) and Foxp3 (FJK-16 s, eBioscience, San Diego, CA) of atherosclerotic lesions at the aortic sinus were performed. Quantitative analysis of MOMA-2, IFN-γ and IL-10-immunostaining were evaluated as a ratio of the positive-stained area to total plaque area in the atherosclerotic lesion. At least three sections per mouse were examined for each immunostaining and appropriate negative controls were used. To evaluate the extent of nonspecific binding in the immunohistochemical experiments, control sections were incubated in the absence of primary antibody. As negative controls of the stainings of IFN-γ and IL-10, aorta of wild type mice were used. To define the subtype of infiltrated macrophages in the atherosclerotic lesions, we analyzed the expression level of CD11c, an M1 macrophage marker [23].

2.4. Quantitative real-time PCR at aortic sinus and whole aorta

At 28 days after first injection, mice were sacrificed under anesthetic condition using pentobarbital sodium (60 mg/kg intraperitoneal injection). The aorta was perfused *in situ* with phosphate buffered saline (PBS), and the whole aorta with aortic sinus was removed. These samples were frozen with liquid nitrogen and stored at -80 °C until each assay. Quantitative real-time PCR (qRT-PCR) analysis for transforming growth factor-β (TGF-β) was performed as described previously [24]. Total RNA was extracted from sample using the RNeasy kit (QIAGEN, Valencia, CA). We used 0.5 µg of total RNA to generate cDNA using the Super Script VILO cDNA synthesis kit (Invitrogen, Carlsbad, CA). qRT-PCR was carried out on a LightCycler system (Roche, Mannheim, Germany) using probes from Universal Probe Library and the TaqMan Master Mix. Sequence of primers and the respective Universal Probe Library probes were as follows: Tgf-beta: forward; CACCATCCATGACATGAACC, reverse; CCGCACACAGCAGTCTTC; IFN-γ: forward; ATCTGGAGGAAGTGGCAA, reverse; CAAGACTTCAAAGAGTCTGAGGTA; IL-10: forward; CAGAGCCACATGCTCC TAGA, reverse; TGTCCAGCTGGTCTTTGTT; Gapdh: forward; TGTCCGT CGTGGATCTGAC, reverse; CCTGCTTACCACCTTCTTG. Relative expression of target genes was calculated with the comparative CT method. Each

Table 1
Body weight and cholesterol levels.

	ApoE ^{-/-}				DKO	
	saline	G-CSF	PC61 saline	G-CSF	saline	G-CSF
Body weight, g	22.7 ± 1.2	22.4 ± 0.8	22.4 ± 0.9	23.6 ± 1.1	24.2 ± 0.6	23.1 ± 0.7
Total cholesterol, mg/dl	3306 ± 171	3527 ± 207	3321 ± 359	3259 ± 245	3767 ± 514	3965 ± 507
HDL cholesterol, mg/dl	29.3 ± 7.3	24.5 ± 4.8	30.8 ± 7.4	28.8 ± 7.5	23.2 ± 6.2	26.2 ± 7.9

HDL indicates high-density lipoprotein. DKO indicates ApoE^{-/-}/CD28^{-/-} double knockout mice. ApoE^{-/-} mice and DKO mice were treated by saline or G-CSF for 28 days. The means ± SEM of 10 animals are shown.

sample was run in duplicate, and the results were systematically normalized using Gapdh.

2.5. Mobilization procedure of Tregs and flow cytometry analysis

Twelve-week-old male C57BL/6 mice received G-CSF at a dose of 200 μg of G-CSF or saline once a day for 5 consecutive days per a week for 4 weeks. At day 28, the total cells of spleen and inguinal lymph nodes were taken and the cell surface phenotype of splenocytes and lymphocytes were analyzed by flow cytometry. All cells were incubated in ice cold PBS supplemented with 3% fetal calf serum and 0.1% azide. One million cells per sample were incubated for 15 minutes at ice cold temperature with the following mAbs: Phycoerythrin (PE)-conjugated anti-mouse CD4 (clone L3T4, BD Biosciences, Le Pont de Claix, France), Fluorescein isothiocyanate (FITC)-conjugated anti-mouse CD25 (clone 7D4, BD Biosciences, Le Pont de Claix, France).

At day 28, the total cells of spleen were taken and the cell phenotypes of lymphocytes were analyzed by flow cytometry. After magnetic

activated cell sorter (MACS) with CD4⁺ antibody and the stimulation with phorbol myristate acetate (PMA) and ionomycin, the cells were incubated with permeabilization buffer and stained with FITC-labeled anti-IFN- γ antibody and PE-labeled anti-IL-4 antibody for analysis with a flow cytometer [19]. CD4⁺IFN- γ ⁺IL-4⁻ cells and CD4⁺IFN- γ ⁻IL-4⁺ cells were defined as Th1 cells and Th2 cells, respectively, and the Th1/Th2 ratio was calculated.

Thirty thousand events were acquired using EPICS ALTRA flow cytometric analysis (Beckman Coulter, Fullerton, CA). Analysis of the acquired data was performed using Expo32 MultiCOMP software (Beckman Coulter, Fullerton, CA).

2.6. Isolation and functional assays of Tregs

Tregs were isolated from spleen cell suspensions by the CD4⁺CD25⁺ regulatory T cell isolation kit (Miltenyi Biotec, Tokyo, Japan), which depletes samples of non-CD4⁺ T cells followed by positive selection of CD4⁺CD25⁺ cells. The purity of the isolated CD4⁺CD25⁺ cells was

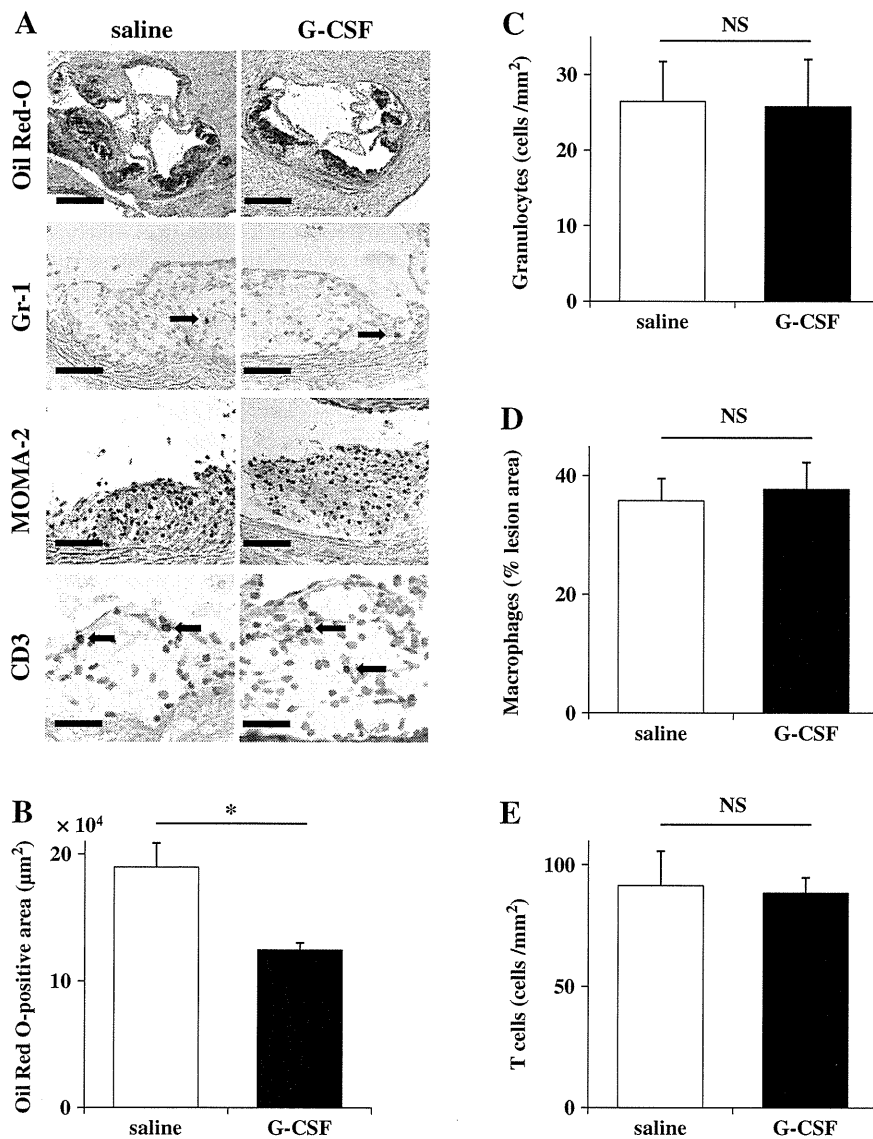
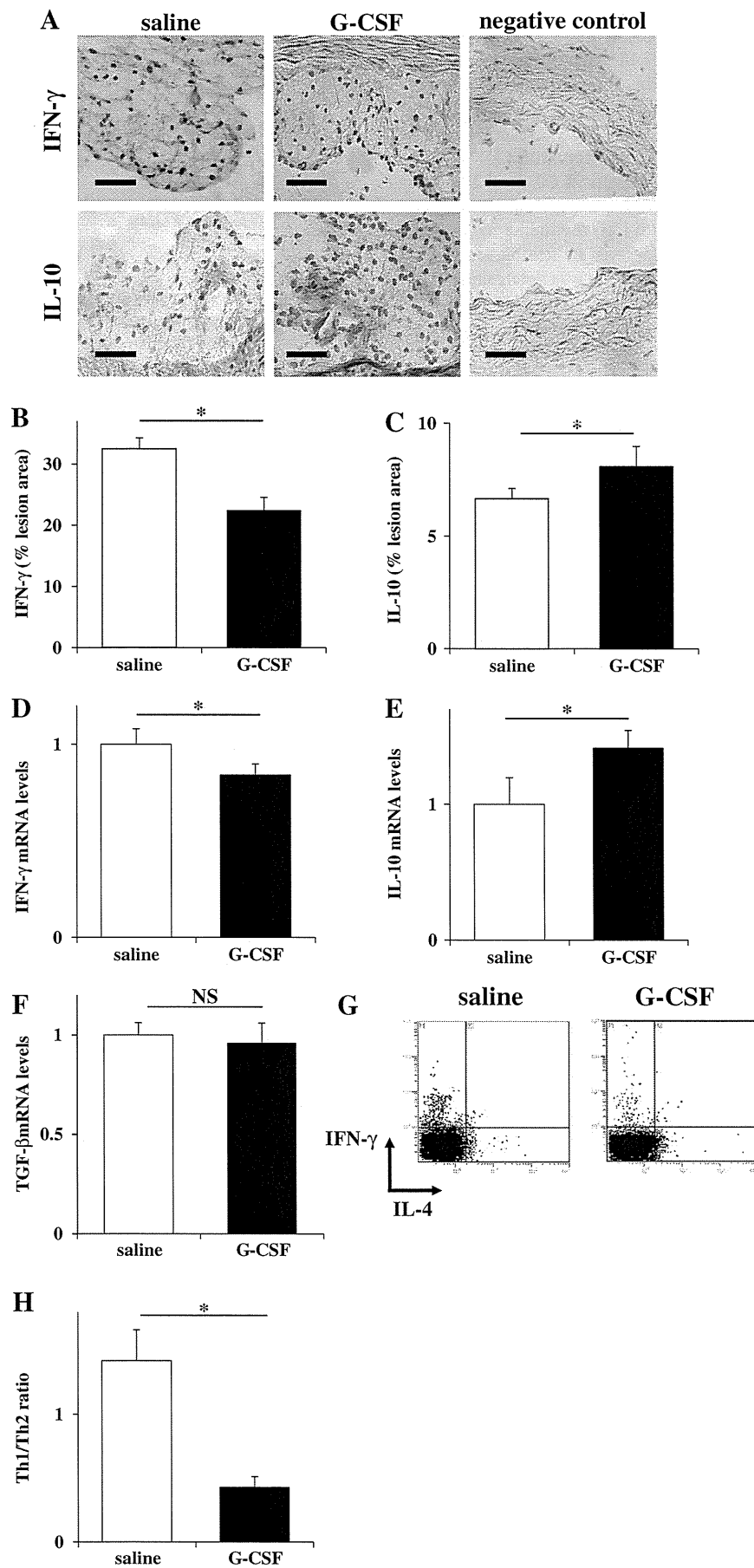


Fig. 1. Effects of G-CSF on atherosclerotic lesions at the aortic sinus in ApoE^{-/-} mice. (A) Representative photographs of atherosclerotic lesion formation (Oil Red-O staining) (Scale bars; 400 μm) and immunostaining of Gr-1 (Scale bars; 100 μm), MOMA-2 (Scale bars; 100 μm) and CD3 (Scale bars; 50 μm) at the aortic sinus of each mouse fed atherogenic diet in the saline group and the G-CSF group. (B) Quantitative analysis of the degree of atherosclerosis at the aortic sinus in both groups. The average lesion area of five sections at the aortic sinus from each mouse was quantified morphometrically as described in Materials and methods. (C) The number of infiltrated granulocytes in the atherosclerotic lesion calculated by immunostaining with Gr-1. (D) The lesion area of infiltrated macrophages in the atherosclerotic lesion calculated by immunostaining with MOMA-2. (E) The number of infiltrated T lymphocyte in the atherosclerotic lesion calculated by immunostaining with CD3. * $P < 0.05$. NS indicates that there is no significant difference between the groups. The means \pm SEM of 10 animals are shown.



>85% by fluorescence-activated cell sorter analysis. All suppression assays were performed in 96-well round-bottom plates in a final volume of 200 μ l/well of RPMI 1640 medium (Sigma-Aldrich, St Louis, MO) supplemented with 10% FCS, 10 mmol/l HEPES, 50 μ mol/l β -mercaptoethanol and antibiotics. Before the assay, 96-well plates were coated with 50 μ l of a final concentration of 10 μ g/ml anti-CD3 (Cedar-Lane Laboratories, Burlington, NC). The CD4⁺CD25⁻ responder cells were plated at 5×10^4 /well alone or in combination with CD4⁺CD25⁺ Tregs at 5×10^4 /well and incubated at 37 °C with 5% CO₂ for 72 h. Then 1×10^5 irradiated (3000 rads) splenocytes were added as antigen-presenting cells. Cultures were pulsed with [³H] thymidine for the last 16 h of culture [25]. Cell proliferation was assayed by scintillation counting (β counter). Percent inhibition of proliferation was determined from the following formula: $1 - (\text{median } [^3\text{H}] \text{ thymidine uptake of } 1:1 \text{ CD4}^+\text{CD25}^+ : \text{CD4}^+\text{CD25}^- \text{ coculture} / \text{median } [^3\text{H}] \text{ thymidine uptake of } \text{CD4}^+\text{CD25}^+ \text{ cells})$.

2.7. Statistical analysis

Data are presented as mean \pm SEM. An unpaired Student *t*-test was used to detect significant differences when two groups were compared. One-way ANOVA was used to compare the differences among four groups with Fisher's PLSD test for post hoc analysis. $P < 0.05$ was considered statistically significant.

3. Results

3.1. Atherosclerosis at aortic sinus

There were no significant differences between the saline- and the G-CSF-treatment groups in body weight, serum total cholesterol and high-density lipoprotein cholesterol levels (Table 1). The degree of atherosclerotic lesion assessed by Oil Red-O staining at the aortic sinus was significantly reduced in the G-CSF-treated mice compared with the saline-treated mice (G-CSF group: $12.4 \pm 0.6 \times 10^4 \mu\text{m}^2$ vs. saline group: $19.0 \pm 1.9 \times 10^4 \mu\text{m}^2$, $P < 0.05$) (Fig. 1A, B). There was no significant change in the number of infiltrated granulocytes in atherosclerotic lesions between the two groups (G-CSF group: 22.1 ± 18 cells/mm² vs. saline group: 23.5 ± 14 cells/mm², $P = 0.87$) (Fig. 1A, C). Immunohistochemical staining on atherosclerotic lesions of aortic sinus revealed that the percentage of cross-sectional area occupied by macrophages (MOMA-2-positive staining) was not significantly different between the two groups (G-CSF group: $37.7 \pm 13\%$ vs. saline group: $35.8 \pm 9.9\%$, $P = 0.75$) (Fig. 1A, D). The ratio of CD11c-positive M1 macrophages to total infiltrated cells was not changed in the atherosclerotic lesions of the G-CSF-treated mice compared to the saline-treated mice (G-CSF group: $8.2 \pm 1.1\%$ vs. saline group: $9.0 \pm 0.5\%$, $P = 0.31$). The number of CD3-positive T cells was not also significantly different between the two groups (G-CSF group: 88.4 ± 19 cells/mm² vs. saline group: 91.5 ± 37 cells/mm², $P = 0.87$) (Fig. 1A, E).

3.2. Effect of G-CSF on cytokine expression

To elucidate the mechanisms by which G-CSF reduced the degree of atherosclerosis, we examined the local cytokine expression in the saline- and the G-CSF-treated mice. Level of proinflammatory cytokine IFN- γ in the atherosclerotic lesions was lower in the G-CSF-treated mice compared with the saline-treated mice (G-CSF group: $22.4 \pm 2.7\%$ vs. saline group: $32.5 \pm 2.2\%$, $P < 0.05$) (Fig. 2A, B). Meanwhile,

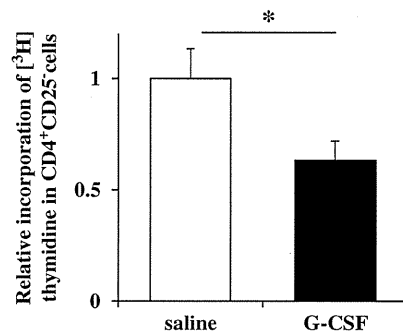


Fig. 3. Effects of G-CSF on the inhibitory function of Tregs. CD4⁺CD25⁻ effector T cells were co-cultured with Tregs from the saline- or the G-CSF-treated mice at the ratio of 1:1 and the incorporation of [³H] thymidine in CD4⁺CD25⁻ cells was counted. * $P < 0.05$. The means \pm SEM of 6 animals are shown.

G-CSF treatment increased the level of antiinflammatory cytokine IL-10 in the atherosclerotic lesions (G-CSF group: $8.1 \pm 0.9\%$ vs. saline group: $6.7 \pm 0.5\%$, $P < 0.05$) (Fig. 2A, C). The expression levels of IFN- γ and IL-10 mRNA were also significantly different between the two groups (IFN- γ ; G-CSF group: $0.8 \pm 0.1\%$ vs. saline group: $1.0 \pm 0.1\%$, $P < 0.05$, IL-10; G-CSF group: $1.4 \pm 0.1\%$ vs. saline group: $1.0 \pm 0.2\%$, $P < 0.05$) (Fig. 2D, E). Since we could not perform TGF- β immunostaining due to technical problems, we examined the expression level of TGF- β mRNA by using qRT-PCR. The expression level of TGF- β mRNA was not significantly different between the two groups (Fig. 2F).

We examined the effects of G-CSF on Th1/Th2 balance. The Th1/Th2 ratio was significantly reduced in the G-CSF-treated mice (G-CSF group: 0.4 ± 0.1 vs. saline group: 1.4 ± 0.2 , $P < 0.01$) (Fig. 2G, H).

3.3. Effect of G-CSF on function of Tregs

To evaluate whether the function of Tregs is influenced by G-CSF treatment, we compared the suppressive function of the Tregs isolated from the saline- and the G-CSF-treated mice. CD4⁺CD25⁺ Tregs from each mouse were co-cultured with CD4⁺CD25⁻ effector cells from wild type mice at the ratio of 1:1 in cell number. Tregs from the G-CSF-treated mice significantly inhibited the incorporation of [³H] thymidine in CD4⁺CD25⁻ effector cells compared with Tregs from the saline-treated mice (Fig. 3).

3.4. Effect of G-CSF on the number of Tregs

To elucidate the mechanism of antiinflammatory effects of G-CSF, we investigated whether G-CSF increases the number of Tregs or not. First of all, we examined the systemic effects of G-CSF on the number of Tregs by flow cytometry analysis of cells from spleen and inguinal lymph nodes of C57BL/6 mice. G-CSF increased the number of CD4⁺CD25⁺ Tregs in spleen (G-CSF group: $249.0 \pm 18.0 \times 10^4$ cells vs. saline group: $88.2 \pm 4.2 \times 10^4$ cells, $P < 0.01$) (Fig. 4A, B) and inguinal lymph nodes (G-CSF group: $54.0 \pm 5.2 \times 10^3$ cells vs. saline group: $31.0 \pm 2.8 \times 10^3$ cells, $P < 0.01$) (Fig. 4A, C).

We next examined whether G-CSF enhances the number of Tregs in atherosclerotic lesions. G-CSF significantly increased the number of Foxp3-positive Tregs in the atherosclerotic lesions of aortic sinus (Fig. 5A, B). The number of Foxp3-positive regulatory T cells was 3.1-fold increased at the atherosclerotic lesions of the G-CSF-treated

Fig. 2. Effects of G-CSF on cytokine levels in atherosclerotic lesion at the aortic sinus. (A) Panels are representative photographs of immunostaining with IFN- γ and IL-10 in the atherosclerotic lesion of the G-CSF-treated mice and the saline-treated mice and the aorta of wild type mice (negative control). (B) Levels of IFN- γ calculated in the atherosclerotic lesion of the G-CSF-treated mice and the saline-treated mice. (C) Levels of IL-10 calculated in the atherosclerotic lesion of the G-CSF-treated mice and the saline-treated mice. (D) Expression levels of IFN- γ mRNA detected by real-time PCR analysis. (E) Expression levels of IL-10 mRNA detected by real-time PCR analysis. (F) Expression levels of TGF- β mRNA detected by real-time PCR analysis. (G) The proportions of CD4⁺IFN- γ ⁺IL-4⁻ cells and CD4⁺IFN- γ ⁻IL-4⁺ cells from spleen of the G-CSF- and the saline-treated mice assessed by flow cytometric analysis. (H) The Th1/Th2 ratio in spleen of the G-CSF- and the saline-treated mice assessed by flow cytometric analysis. * $P < 0.05$. NS indicates that there is no significant difference between the two groups. Scale bars indicates 50 μ m. The means \pm SEM of 10 animals are shown.